123

On the Measurement of the Resistivity in an Exploding Wire Experiment

Luis Bilbao, Gonzalo Rodríguez Prieto

***Abstract*—Explosion of a metallic wire due to a large electrical current can be used for studying metallic states difficult to reach with other methods. Due to experimental constraints, direct measurement of the voltage drop across the wire is impractical, although many characteristics of the metal state in the wire can be derived from these waveforms. Usually, the transformation of the electrical signals is made with the assumption of a lumped model for all the elements of the circuit, including the wire. We discuss the validity of a lumped model, and we show that due to the variation in time of the current density distribution on the wire, this model will not provide accurate values for the wire resistivity. Wire resistivity inaccuracies are specially clear in gas and plasma states, due to the diffusion and movement of the current that produce a large variation of the magnetic flux inside the wire.**

In order to obtain more precise results in the resistivity of the wire metal, regardless of its state, a better approach is the use of the Faraday's law of induction on a path along the border of the wire. Our experiments of exploding wires in atmospheric air present the advantage of the clear electrical boundary between the expanding wire and the surrounding air, where no current circulates. As the state of the wire boundary layer changes form solid to plasma, it is possible to estimate the resistivity of the metal in those states in a more precise way.

***Index Terms*—Circuit analysis, metals, atmospheric-pressure plasmas, exploding wire, resistivity.**

I. INTRODUCTION

WHEN a large electrical current passes through a metallic wire of the proper dimensions, typically 100 µm of diameter and centimeters length, the metallic wire is heated rapidly by Joule effect, becoming liquid, then gas, to later be transformed in plasma. This system is called exploding wire, and it is well known to science since a long time. It had been used in multiple endeavors, because the rich phenomena that can be accessed with it. Broad examples of the use of exploding wire are the general use as generator mechanism for blast waves [1] or the better understanding of the fuse dynamics through experiments like in the work of Vermij [2]. Exploding wire systems can also be used for important industrial or military applications, like in the preparation of metallic nano-powders reviewed by Kotov et al. [3], or the study of the mitigation of blast waves by foam, through the use of a surrogate setup, as in the recent work of Liverts et al. [4].

L. Bilbao is with Universidad de Buenos Aires, Facultad de Ciencias Exactas, Departamento de Física, Buenos Aires, Argentina and CONICET, Infip, Buenos Aires, Argentina.

G. Rodríguez Prieto is with Universidad de Castilla-La Mancha, Spain and INEI, Ciudad Real, Spain

Manuscript received ...; revised ...

In order to create the high current necessary for this phenomenon, large capacitors and high voltages are necessary in the electrical circuit that delivers the current to the wire load. Main circuit characteristics, like the total inductance, resistance and capacitance due to the capacitor bank, can be well modeled by a RLC model, while the spark-gap and the wire need a different model.

Experimental voltage waveforms are usually obtained from probes attached to the circuit. Due to experimental constrains, sometimes the voltages probes are not exactly placed between the wire extremes, but separated by fixed circuit elements from them, for example, as described in the experimental works [5]–[9].

Additionally, there is a problem with the modeling of the experimentally obtained voltage and current signals, in the sense that the exploding wire electrical characteristics must be included in this modeling. In order to interpret experimental measures of current and voltage and, therefore, resistance or other electrical parameters, some authors use simple models assuming the wire as a lumped element. With this approach, the resistance of the wire, and in later stages, of the plasma, can be measured indirectly using the voltage signals, as in [10]–[13].

Despite the broad use of the lumped model for the wire, the description is not accurate during the time when the diffusion of the electrical current is important or when a large variation of the resistivity occurs within the wire. For example, Z–pinch system dynamical evolution, in which a cylindrical array of wires are made to implode radially by the gradient of the self-magnetic field of the current flowing through the wire array, cannot be described by just a lumped model for every wire [14], [15]. In fact, it was already noticed that in such systems, the plasma spatial and temporal distribution around every wire following the first moments of the electrical discharge is important in the dynamical description of the Z–pinch [16], [17].

So, a description of the exploding wire circuit, accounting for the distributed nature of the phenomenon, is important to understand and better qualify the wire explosion by means of an intense electrical current. Therefore, we present here a different approach to the description of the circuit. It is based on the derivation of the circuit equation by means of the Faraday's law of induction.

II. ELECTRICAL CIRCUIT

The experimental setup of ALEX (ALambre EXplosivo, exploding wire acronym in Spanish), the exploding wire experiment motivating this work, including an optical streak camera, has been described in a previous work [18]. Nevertheless, it is worthwhile to recall here a description of its electrical circuit and the associated probes. The capacitor bank, two parallel Castor oil capacitors of 1.1 μF each, is charged by a high voltage source of a maximum voltage of 65 kV. Upon arrival to the desired nominal voltage, the high voltage source is disconnected from the circuit, and the spark-gap is triggered (see fig. 1). Later on, when the spark-gap switch is fully closed, the circuit is equivalent to a RLC circuit plus the wire load. Wire was made of Copper, with a length of 31 mm and diameter of 50 μm.

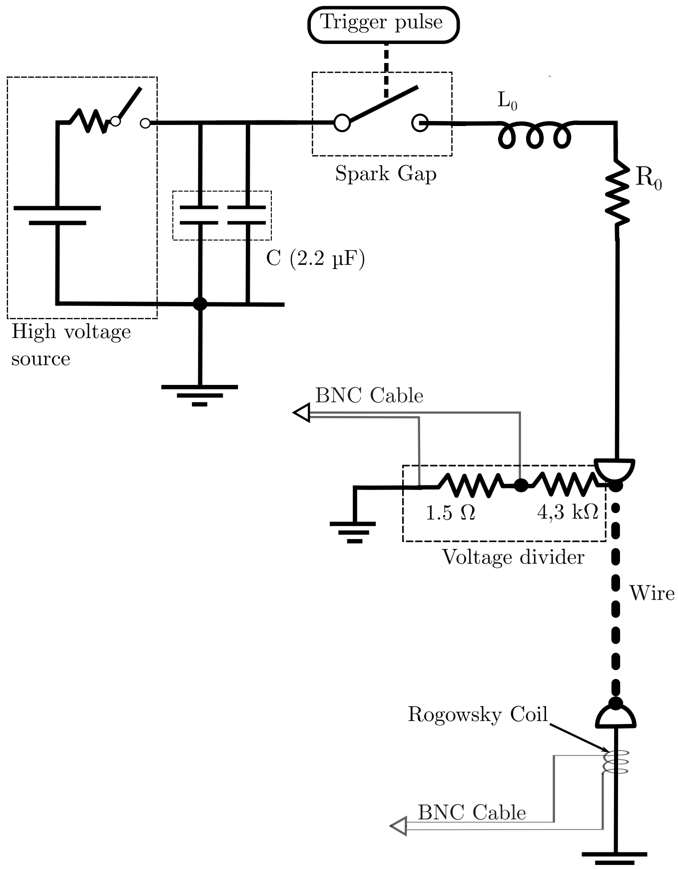

Fig. 1. ALEX electrical scheme. R_0, L_0 and C represent the lumped circuit resistance, inductance and capacitance, respectively. Open arrows indicate the BNC connections to the oscilloscope.

The use of lumped element model for the exploding wire is not always the best approach. The discharge on the wire produces a current that diffuses due to its resistivity. During this stage, it is impossible to define separately a resistance and an inductance as lumped parameters of the circuit [19]. Notwithstanding this fact, lumped element models for the wire have been used for more than 50 years [6], [20]–[22], and, therefore, it is a common practice to refer to resistance and inductance of the wire. The practical use of such approach is justified as a way for obtaining the resistivity of the metal as a function of time from the electrical signals and the wire/plasma radius evolution. An example, which clearly states this lumped model for the wire, is the work of Sasaki et al. [10]. Be aware that the above model is not of general application because it requires a homogeneous evolution in density and resistivity.

The above hypothesis is not usually well justified in all the stages of the exploding wire evolution. For example, just after the initial rise of electrical current, its value drops almost to zero while the full voltage is across the wire. This low current stage, called dark pause, lasts for a given time until a second surge of the current develops, see fig. 2, and under appropriate conditions it can last several μs.

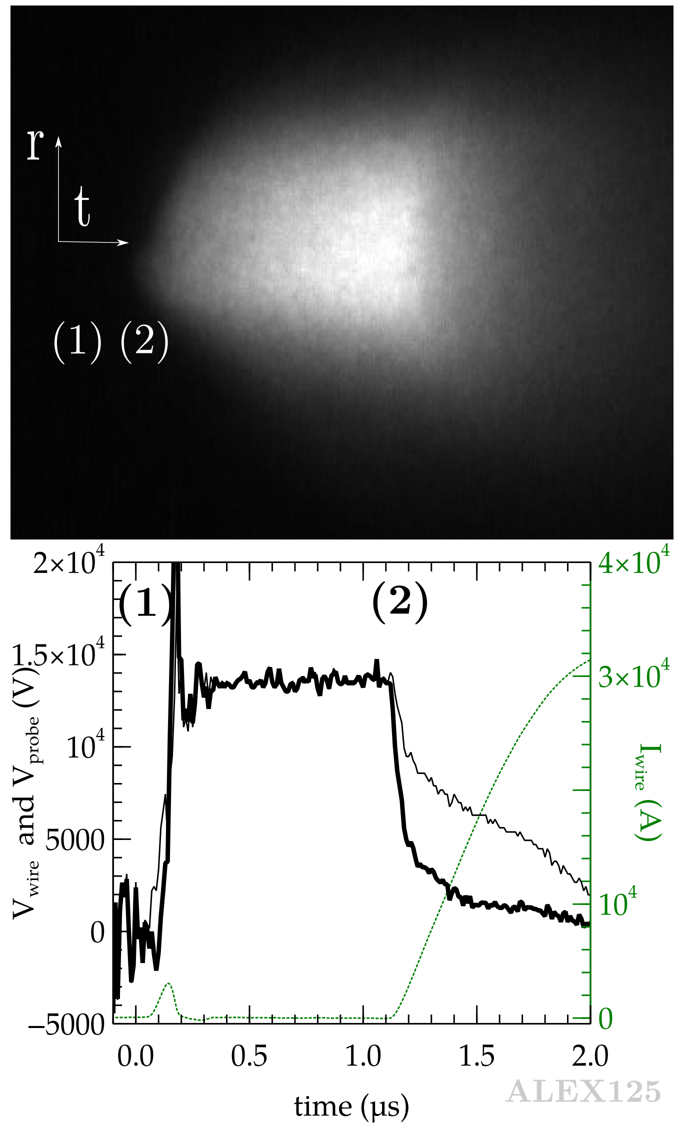

Fig. 2. (Color Online) In the upper panel, exploding wire streak image is shown. Time in the horizontal axis is 20 μs, and space in the vertical axis, 24 mm. Bottom panel shows the voltage through the wire (**—**), the signal of the voltage probe (—), and the current (···). Note that current during the dark pause is different from zero. Numbers in both panels corresponds approximately to the same moments in both the streak image and the signals. Charging voltage was 15 kV with a wire diameter of 50 μm.

The elapsed time between the first and the second surges of the current will depend on the resistivity of the wire and the distribution of the current. The wire is heated by Joule effect, and from the energy given to the wire system, we find that after the first current surge the wire melts and later on, its external layer starts to vaporize. When part of the wire vaporizes, the sudden increase of the wire resistivity produces a sharp drop in the current. Although small, a residual current continues flowing and heating up the wire and a vaporization wave progresses through the wire. This means that different states (liquid, liquid/gas, and gas) may coexist in the wire, having very large difference in their resistivities. Indeed, the experimental parameters were chosen to allow for the exploration of classical states of matter in thermal equilibrium, in sharp contrast with more usual exploding wire experiments, aimed to explore warm dense matter conditions.

The use of one phase homogeneous model like the used in [10] is inadequate in our experimental conditions, where the dark pause stage is characterized by a large current diffusion at the beginning and the end, in addition to a two different homogeneous phases, an inner liquid surrounded by an expanding gas, during the remaining time of quasi constant current. Thus, a lumped element model of this stage will not be of sufficient accuracy to evaluate the Joule heating contribution to metallic gas. In order to increase the accuracy and allow for a better quantitative estimation of the gas resistivity, a model for the electrical circuit, based on Faraday's law of induction, that considers the wire as an extended entity is described in the next section.

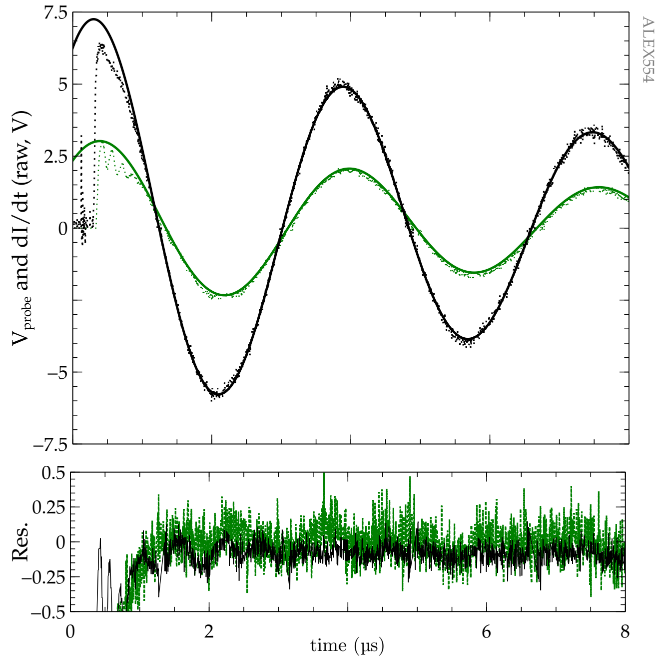

Fig. 3. (Color Online) ALEX short circuit current derivative and voltage raw waveforms and their fit (top panel) with the residual (down panel) when charged at 10 kV. Rogowski probe voltage experimental (···) and fit (—) values are black lines, meanwhile voltage divider experimental (···) and fit (—) traces are depicted in green in both panels. Note the large value of the residual at the beginning of the discharge, when an oscillation is produced by the finite closure time of the spark-gap.

III. CIRCUIT EQUATION

In order to model the electrical circuit, it is divided into three distinct parts: a) capacitors, cables, electrodes and connections, b) the spark-gap, and c) the exploding wire.

Part a) can be modeled with a RLC lumped element model, as it is experimentally seen using a short circuit. In our case, the wire is removed and the cathode is displaced until it touches the anode, i.e. no short circuit element is added.

On the one hand, the measured current derivative, dI/dt, can be perfectly fitted by a damped cosine at the later stage where the voltage drop across the spark-gap is zero. The values of the lumped elements R_0 and L_0 are obtained from the fit with high precision, see fig. 3 (the capacitance, C, is provided by the manufacturer). The difference between the fitted RLC signal and the actual signal that is seen at the beginning of the signal (the first µs in fig. 3) is an oscillation due to the finite closure time of the spark-gap.

On the other hand, the measured voltage (i.e. the voltage drop in the cathode, when no wire is present) is perfectly fitted by a lumped resistance, $R_{cathode}$, and inductance, $L_{cathode}$. These values (different from R_0 and L_0) are obtained using a multiple linear regression of V_{probe} on dI/dt and the current I (obtained by numerically integrating dI/dt) by noting that, under short circuit conditions,

$$V_{probe} = R_{cathode} I - L_{cathode} \frac{dI}{dt}. \quad (1)$$

The fitted signal of the voltage probe and its residual are also plotted in fig. 3.

Due to the fact that the closure time of the spark-gap is much shorter than the period of the discharge, the behavior of the spark-gap, part b), is well modeled by a variable voltage drop. For the voltage variation across the spark-gap, $V_{sg}(t)$, we have used [23]

$$V_{sg}(t) = \frac{2V_0}{1 + \exp(t/\tau)}, \quad (2)$$

where V_0 is the initial charging voltage of the capacitor, τ the spark-gap closure time (30 ns in our case), and $t = 0$ corresponds to the trigger of the spark-gap.

To model the exploding wire, part c), we start by assuming that the current is not homogeneous across the wire section, that is, the current is distributed in space, and therefore flows through different paths between the electrodes.

Usually Kirchhoff's circuit laws are used to solve the current and voltage in an exploding wire experiments, regardless that it is only valid for a lumped element model. When the current is spatially distributed a more precise way to write the circuit equation is by means of the Faraday's law of induction, along a closed path across the full circuit, that goes through the lumped elements, the spark-gap, and the exploding wire as

$$\frac{d\Phi}{dt} = -\oint \mathbf{E}' \cdot d\mathbf{l}, \quad (3)$$

where Φ is the magnetic flux enclosed by the path, and $\mathbf{E}'$ the electric field in a system fixed to the path ($d\mathbf{l}$). The path may be a material or an immaterial one. Also, it may be a fixed or a mobile path relative to the lab system. In any case the electric field $\mathbf{E}'$ is evaluated in a system fixed to the path, not to the lab.

Along the part modeled with the lumped element model, the path is unique (i.e., lumped elements have no thickness), while on the exploding wire (whether on its initial state or during its evolution) any path that connects the electrodes may be used.

The integration of the electric field on the part that is modeled by a lumped element is straight forward, because it holds that

$$\int_{inductance} \mathbf{E}' \cdot d\mathbf{l} = L_0 \frac{dI}{dt}, \tag{4}$$

$$\int_{resistance} \mathbf{E}' \cdot d\mathbf{l} = R_0\, I, \tag{5}$$

and

$$\int_{capacitor} \mathbf{E}' \cdot d\mathbf{l} = -\frac{Q}{C}, \tag{6}$$

where Q is the charge.

On the other hand, as it was mentioned above, the spark-gap can be modeled by a variable voltage, that is

$$\int_{spark-gap} \mathbf{E}' \cdot d\mathbf{l} = V_{sg}\left(t\right). \tag{7}$$

Finally, for the exploding wire it is necessary to choose a path that connects the electrodes. For example, using path a as shown in fig. 4, left panel, (3) becomes

$$\frac{d\Phi_a}{dt} + \int_a \mathbf{E}' \cdot d\mathbf{l} = \frac{Q}{C} - R_0 I - L_0 \frac{dI}{dt} - V_{sg}\left(t\right), \tag{8}$$

where Φ_a is the magnetic flux enclosed by the whole circuit that is closed by the path a in the wire. Any other path may be used as well, including a mobile path along the wire boundary (see fig. 4, central panel), in which case we have

$$\frac{d\Phi_b}{dt} + \int_b \mathbf{E}' \cdot d\mathbf{l} = \frac{Q}{C} - R_0 I - L_0 \frac{dI}{dt} - V_{sg}\left(t\right). \tag{9}$$

Clearly, (8) and (9) produce the same voltage drop in the circuit, since Faraday's law along a closed path formed by a and b, gives

$$\frac{d\Phi_a}{dt} + \int_a \mathbf{E}' \cdot d\mathbf{l} = \frac{d\Phi_b}{dt} + \int_b \mathbf{E}' \cdot d\mathbf{l}. \tag{10}$$

(see fig. 4, right panel).

The above relationship also shows an important fact when diffusion of the current is the dominating phenomenon: it is impossible to meaningfully define separately a resistance and an inductance of the wire as lumped parameters in the circuit [19]. This can be better seen using the Ohm law in a system fixed to the wire material, where the electric field is evaluated, that is

$$\mathbf{E}' = \rho\mathbf{j}, \tag{11}$$

where ρ is the resistivity and $\mathbf{j}$ the current density, then (10) becomes

$$\frac{d\Phi_a}{dt} + \int_a \rho\mathbf{j} \cdot d\mathbf{l} = \frac{d\Phi_b}{dt} + \int_b \rho\mathbf{j} \cdot d\mathbf{l}. \tag{12}$$

Equation (12) shows that the inductive (first terms in each side) and the resistive parts (second terms in each side) depend on the path, thus a unique definition of the total inductance and resistance of the wire can not be made unless a uniform current density distribution is present. The assumption of an uniform radial distribution of the current in the wire cross-sectional area is not valid when the diffusion time of the magnetic field of the current is shorter than the typical time scale of the process. Also, there is another fact that prevents from having an uniform current density distribution even in the long time scale. In our experiments a liquid core coexists with a surrounding metallic gas. The large difference in the resistivity of both phases produces a large difference in the current density therefore, the radial distribution is not uniform in the long time scale (microsecond in our experiments). Therefore, we are not allowed to use the hypothesis of current density uniformity in these calculations.

Although (8) and (9) can be used interchangeably, we have chosen the path b along the border of the wire. Assuming cylindrical symmetry, the azimuthal magnetic field B outside the border of the wire is

$$B = \frac{\mu_0 I}{2\pi r_b}, \tag{13}$$

where r_b is the radius of the border and I the total current circulating through the wire, that is also related to the integration of the current density through the section ($d\mathbf{S}$) of the wire as

$$I = \int \mathbf{j} \cdot d\mathbf{S}. \tag{14}$$

Note that the electrical current does not circulate beyond the wire border because of the air surrounding the wire. Thus, the calculation of the magnetic flux enclosed by a path along the border of the wire and the returning plate, can be simply calculated as

$$\Phi_b = L_b I,$$

being L_b a geometrical relationship equivalent to an inductance. In our device, the returning electrical path is a conducting plate separated by a distance d from the axis of the wire, in which case L_b can be approximated by

$$L_b = \frac{\mu_0 l}{2\pi} \cosh^{-1}\left(\frac{d}{r_b}\right), \tag{15}$$

where l is the length of the wire. Therefore, (9) becomes

$$\frac{d\left(L_b I\right)}{dt} + \int_b \rho\mathbf{j} \cdot d\mathbf{l} = \frac{Q}{C} - R_0 I - L_0 \frac{dI}{dt} - V_{sg}\left(t\right), \tag{16}$$

Note that L_b cannot be considered as the wire inductance, since further magnetic flux that varies with time is inside the wire. Similarly, the second term of the left hand side of (16) cannot be replaced by a lumped resistance voltage drop in the form $R_b I$. Making such substitution implies that the terms R_b and dL_b/dt will be undistinguished between them in the electrical signals, thus a unique solution for R_b can not be experimentally obtained. This fact has been pointed out by Fridman [24] in the sense that time evolution of the resistance and the inductance obtained from the oscillograms of current and voltage is not a single-valued problem.

Actually, there is no need of calculating a wire inductance or resistance in order to solve the circuit equation. Instead, a "boundary inductance" (L_b) and a "boundary resistive voltage drop" ($\int_b \rho\mathbf{j} \cdot d\mathbf{l}$) are sufficient. Inside the wire, the Faraday's law of induction may be further used for deriving its structure,

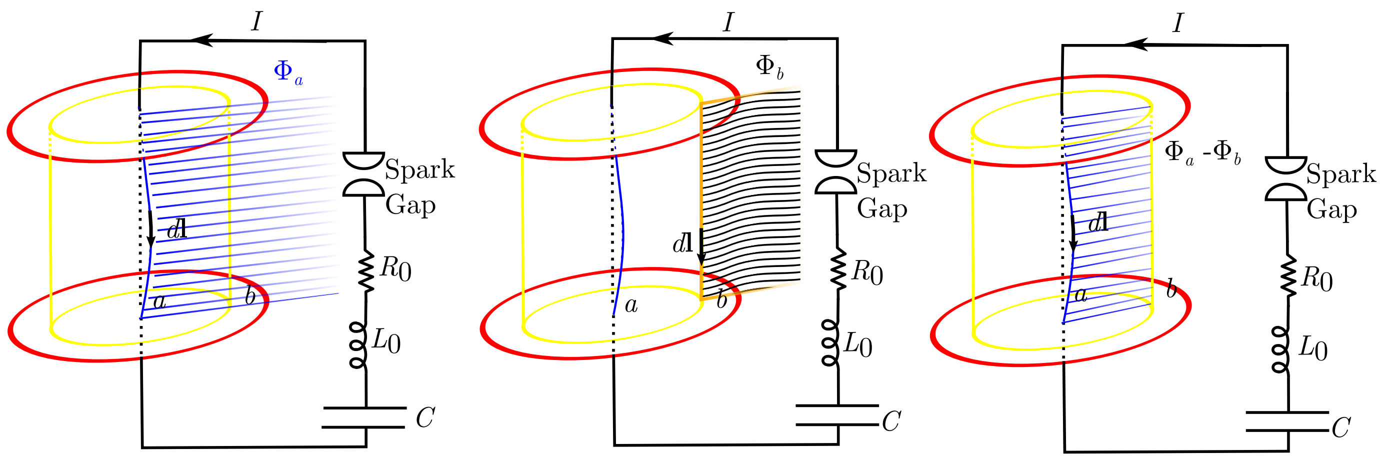

Fig. 4. (Color Online) ALEX integration paths with an schematic representation of the magnetic flux through the circuit produced by the wire explosion. Left panel indicates the path through the center of the plasma, central panel through the outer border of the plasma, and in the right panel, the flux difference between previous paths.

as in (12).

The set of equations (16) and (15) plus the exploding wire evolution, together with the initial conditions

$$Q\left(t=0\right)=CV_0\ ; \qquad I\left(t=0\right)=0\ ; \qquad \frac{dI}{dt}\left(t=0\right)=0$$

solves the circuit.

From an experimental point of view, it is possible to obtain information on the resistivity, from the voltage drop on the wire, left hand side of (16), which is:

$$V_{wire}=\frac{d\left(L_b I\right)}{dt}+\int_b \rho\mathbf{j}\cdot d\mathbf{l}. \tag{17}$$

Under cylindrical symmetry, i.e. assuming no axial dependence, the above becomes

$$V_{wire}=\frac{d\left(L_b I\right)}{dt}+\rho_b j_b l, \tag{18}$$

where ρ_b and j_b are the resitivity and current density in the border of the wire, respectively.

From (18) the resistivity of the boundary layer can be obtained from the electrical signals as long as the current density in the border, and the movement of the boundary layer are also known.

In our experiment, for the measurement of the voltage drop on the wire, we have to take into account that the position of the voltage divider is at the connection between the anode and the wire, as it was previously mentioned. Therefore, the measured voltage drop, V_{probe}, is the sum of the voltage drop across the exploding wire, V_{wire}, plus the voltage drop in the cathode and connections, therefore

$$V_{wire}=V_{probe}-R_{cathode}I-L_{cathode}\frac{dI}{dt}, \tag{19}$$

where the current I is obtained by numerically integrating dI/dt, which is measured with the Rogowski coil.

IV. Numerical simulation

The aim of the numerical simulation is to help to understand the influence of the magnetic flux variation and the nonuniform resistivity inside the wire in the interpretation of electrical signals.

During the dark pause the drop of the current indicates an important increment of the resistivity. The variation of resistivity of the copper until the boiling temperature [25] is not high enough to explain the observed drop, suggesting that the wire has been partially vaporized, because the energy provided to the wire up to this time, is not enough to vaporize the whole wire.

The end of the dark pause occurs when the metallic gas is ionized and the current is re-establish through the wire. Note that for simplicity we call "wire" to any state, that is solid, liquid, gas or plasma.

In order to show this idea, a 1D numerical code has been used to simulate the exploding wire dynamics. A key hypothesis in this approach is the symmetry of the wire evolution during the time of interest, that is the dark pause in the present work. To the purpose of the present analysis, the symmetry of the wire observed during the dark pause by means of streak and framing pictures, allows us the use of a 1D code where magnitudes depend only on the radial coordinate. Therefore, we assumed cylindrical symmetry with only radial dependence. In this way the plasma expansion can be approximate by a 1D system where the spatial coordinate corresponds to the radius.

We have adapted a previous developed 3D code [26], that has been used to simulate different physical problems such as double-base chemical propellant combustion, ignition and propagation of a thermonuclear detonation wave, and, the development of the Kelvin-Helmholtz (KH) instability in the magnetopause. In the present version, a Mie-Grüneisen equation of state for solid and liquid was used, and the ionization state was obtained from a Saha equation. This is justified in the fact that our focus is the study of the dark pause, that ends when a cold plasma is formed. The successive evolution of the plasma at higher temperatures is out of the scope of this study. The code solves the equations of continuity, momentum, and energy plus Maxwell's equations in the wire, coupled to the circuit equation (16) with conditions (13) and (14). The electrical resistivity of copper is readily available for solid, liquid [25] and plasma states, but not for the gas state.

Pressure and density of the gas state are obtained from the radial expansion in time, observed with the streak camera. Estimating the pressure with the Rankine–Hugoniot relationship for the shock into the air at atmospheric pressure and ambient temperature gives values between 10 and 100 atm. In combination with direct measurements of the radius of the expanded gas, a fairly constant density on the order of 5×10^{18} cm^{-3} is estimated. Further, due to the absence of radiation coming from it, we can conclude that the metallic gas is in classical neutral state which resistivity is expected to depend on the gas temperature.

As a first approach we have used an ad hoc linear variation of the resistivity, ρ_{gas}, with the temperature as:

$$\rho_{gas} = \rho_0[1 + \alpha\,(T - T_{boil})], \tag{20}$$

being T the gas temperature in Kelvin, and $T_{boil} = 2940$ K the boiling temperature of copper.

As an starting point for the determination of the parameters, ρ_0 and α, an order of magnitude value was experimentally obtained from the “boundary resistive voltage drop” mentioned above. Then, using the code, the parameters were iterated until a fairly good reproduction of the measured voltages and currents through the wire were obtained. It has been observed that the mean value of ρ_{gas} is related to the dark pause duration, while the slope accounts for the variations of the current and voltage in time.

This procedure was repeated for various initial charging voltage values. The best estimates, using this rough method, were $\rho_0 = 4\times10^{-3}\ \Omega\cdot\mathrm{m}$ and $\alpha = 0.00045/\mathrm{K}$.

The above estimates are intended only to illustrate the differences that may arise when a lumped model is used for the exploding wire. They cannot be taken as a precise value of the copper gas resistivity.

The simulated electrical signals were obtained by solving the numerical code coupled to the circuit equation, using the values of our experiment, $C = 2.2$ µF, $L_0 = 142$ nH, $R_0 = 5$ mΩ, $V_0 = 15$ kV, copper wire 50 µm in diameter and 31 mm long. Fig. 5 shows the voltage drop in the wire (simulated and measured) as a function of time, with the state of the outer layer of the wire over-imposed, as it evolves from solid to plasma. We observed (not shown in the figure) that the state in the inner part of the wire differs from that of the external layer. This means, that different states coexist in concentric layers that evolve with different time scales.

V. Measurement of the Resistivity

As it was mentioned in the Introduction, several authors obtain a value of resistance, R, from the electrical signal, by subtracting the “inductive” part from the voltage drop on the exploding wire as

$$R = \frac{V_{wire} - \frac{d(L_b I)}{dt}}{I}, \tag{21}$$

From (21) a mean resistivity my be inferred as

$$\langle\rho\rangle = \frac{RS}{l}, \tag{22}$$

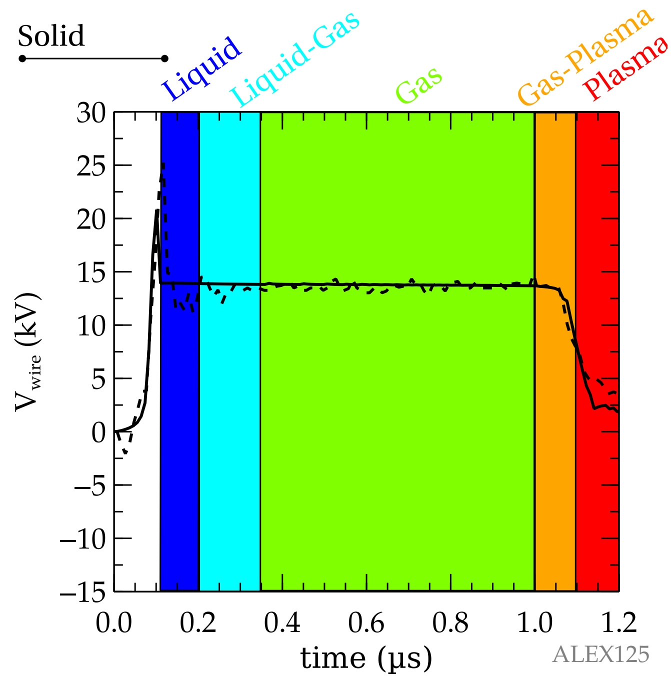

Fig. 5. (Color online) ALEX voltage waveforms (calculated: full line, measured: dashed line) with the states of the outer shell of the wire clearly indicated, for a copper wire with a diameter of 50 μm and with capacitors charged at 15 kV.

where l is the length and S the section of the wire.

Comparing with (18) and assuming cylindrical symmetry it follows that

$$\langle\rho\rangle = \rho_b \frac{j_b}{\langle j\rangle}, \tag{23}$$

where $\langle j\rangle = I/S$ is the mean current density. Clearly, when no magnetic flux variation is inside the wire (this implies that there is no current diffusion, either), the above relationship gives a reasonable mean value since $\rho j = const$ along the radius, unless large variation of the resistivity occurs inside the wire (for example, when different states coexist), in which case, a mean value has no significance.

Using the numerical code, a mean “measured” resistivity, (22), was calculated and compared to a spatial mean resistivity, $\overline{\rho}$, over the radial coordinate, defined as

$$\overline{\rho} = \frac{1}{r_b}\int_0^{r_b} \rho\,(r)\,dr. \tag{24}$$

Other mean values may be defined as well, but the aim of this paper is to show the difficulty in interpreting (22) as a representative value.

The percentage difference $\left(\langle\rho\rangle - \overline{\rho}\right)/\overline{\rho}$ is plotted in fig. 6. As can be seen, the difference varies up to $\pm100\%$. From this result it is clear that the resistivity experimentally obtained from (21) and (22) may considerably depart from the actual value. In the present example it is due to two main factors: a) the diffusion of the current, and b) the different states that simultaneously coexists in the wire.

The effect a) is clearly seen when the current varies in a characteristic time smaller or similar to the diffusion time, as it happens at the beginning and at the end of the dark pause. At the beginning of the electrical discharge, the current density reaches its largest value in the wire surface due to the current concentration in this region, and diffuses to the center of the wire. When the current diffuses from the boundary to the center, the current density is maximum at the border (i.e. $j_b > \langle j \rangle$) producing an overvalued mean resistivity, $\langle \rho \rangle$, as can be seen from (23) and is shown in the initial times in fig. 6. The opposite happens when the current diffuses from the center to the boundary, or similarly when the magnetic flux decreases inside the wire (for example, due to a sudden expansion).

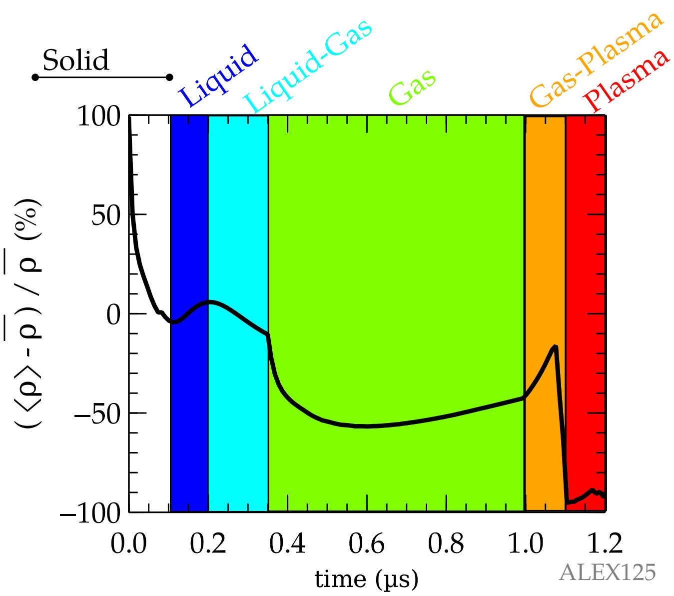

Fig. 6. (Color Online) Calculated percentage resistivity difference between (22) and (24). A copper wire of 50 μm diameter and 30 mm length, charged at 15 kV was used in the simulation. Background color correspond to the outer layer state, as in the previous figure.

As it was mentioned above, in the example of fig. 6, simulations have shown that the gas state of the outer layer coexists with the liquid state of the central layer (not shown in the figure). The coexistence of different states that evolve during the dark pause, produce a large difference of the resistivity (many orders of magnitude) across the wire making meaningless the concept of a mean resistivity such as (22).

VI. Conclusions

Calculation of resistivity from the experimental measurements of the electrical signals and the wire evolution, assuming a lumped element model as in (21) and (22), may give large difference relative to the actual resistivity, in particular, when the current varies during a time comparable to the diffusion time, or when different states coexist inside the wire. Therefore, the use of lumped element model for the exploding wire is at best an approximation, that may be use with care.

If the study of metal properties as a function of temperature and density is seek, a better strategy would be to obtain the resistivity of the outer layer of the wire by measuring the "boundary resistive voltage drop". The external part of the wire varies its state from solid to plasma, thus, in principle, the time variation of the resistivity corresponding to different states may be studied. The resistivity of the outer layer can be estimated, as long as the current density is known.

There is no need to estimate the resistivity of the inner part, nor its mean value on the wire. It is enough to study the outer layer, and, if possible, by also measuring temperature, density and current density.

It is worth mention that the measurements here presented assume the existence of thermal equilibrium, a condition not always achieved in such a dynamic environment as it is the exploding wire. In absence of this local thermal equilibrium condition, the obtained resistivity cannot be understood as any constitutive property of the exploding wire matter, independently of its phase, neutral gas or plasma. Nevertheless, the main objective of this work is the resistivity measurement method for local thermal equilibrium systems, not the determination of non-equilibrium states properties.

References

[1] K. Oshima, "Blast waves produced by exploding wire," Aeronautical Research Institute, University of Tokio, Tech. Rep. 358, 1960.
[2] L. Vermij, "The voltage across a fuse during the current interruption process," *IEEE Transactions on Plasma Science*, vol. 8, no. 4, pp. 460 – 468, 1980.
[3] Y. A. Kotov, "Electric explosion of wires as a method for preparation of nanopowders," *Journal of Nanoparticle Research*, vol. 5, no. 5, pp. 539 – 550, 2003.
[4] M. Liverts, O. Ram, O. Sadot, N. Apazidis, and G. Ben-Dor, "Mitigation of exploding-wire-generated blast-waves by aqueous foam," *Physics of Fluids*, vol. 27, no. 7, p. 076103, 2015.
[5] R. J. Thomas and J. R. Hearst, "An electronic scheme for measuring exploding wire energy," *Instrumentation and Measurement, IEEE Transactions on*, vol. 16, no. 1, pp. 51 – 62, 1967.
[6] A. W. DeSilva and J. D. Katsouros, "Electrical conductivity of dense copper and aluminum plasmas," *Physical Review E*, vol. 57, no. 5, pp. 5945 – 5951, 1998.
[7] D. B. Sinars, M. Hu, K. M. Chandler, T. A. Shelkovenko, S. A. Pikuz, J. B. Greenly, D. A. Hammer, and B. R. Kusse, "Experiments measuring the initial energy deposition, expansion rates and morphology of exploding wires with about 1 ka\wire," *Physics of Plasmas*, vol. 8, no. 1, pp. 216 – 230, 2001.
[8] K. M. Chandler, D. A. Hammer, D. B. Sinars, S. A. Pikuz, and T. A. Shelkovenko, "The relationship between exploding wire expansion rates and wire material properties near the boiling temperature," *IEEE Transactions on Plasma Science*, vol. 30, no. 2, pp. 577 – 587, 2002.
[9] S. Sahoo, A. K. Saxena, T. C. Kaushik, and S. C. Gupta, "Effect of energy deposition rate on plasma expansion characteristics and nanoparticle generation by electrical explosion of conductors," *High Energy Density Physics*, vol. 17, no. B, pp. 270 – 276, 2015.
[10] T. Sasaki, M. Nakajima, T. Kawamura, and K. Horioka, "Electrical conductivities of aluminum, copper, and tungsten observed by an underwater explosion," *Physics of Plasmas*, vol. 17, no. 8, p. 084501, 2010.
[11] D. Sheftman and Y. E. Krasik, "Evaluation of electrical conductivity and equations of state of non-ideal plasma through microsecond timescale underwater electrical wire explosion," *Physics of Plasmas*, vol. 18, no. 9, p. 092704, 2011.
[12] J. Stephens, J. Dickens, and A. Neuber, "Semiempirical wide-range conductivity model with exploding wire verification," *Physical Review E*, vol. 89, no. 5, p. 053102, 2014.
[13] A. Vanderburg, F. Stefani, A. Sitzman, M. Crawford, D. Surls, C. Ling, and J. McDonald, "The electrical specific action to melt of structural copper and aluminum alloys," *IEEE Transactions on Plasma Science*, vol. 42, no. 10, pp. 3167 – 3172, 2014.
[14] S. V. Lebedev, S. N. Bland, J. P. Chittenden, A. E. Dangor, M. G.Haines, K. H. Kwek, S. A. Pikuz, and T. A. Shelkovenko, "Effect of discrete wires on the implosion dynamics of wire arrays Z pinches," *Physics of Plasmas*, vol. 8, no. 8, pp. 3734, 2001.
[15] M. G. Haines, "A heuristic model of the wire array Z–pinch," *IEEE transactions on plasma science*, vol. 26, no. 4, pp. 1275–1281, 1998.

[16] J. P. Chittenden, S. V. Lebedev, A. R. Bell, R: Aliaga–Rossel, S. N. Balnd, and M. G. Haines, "Plasma formation and implosion structure in wire array Z pinches," *Physical Review Letters*, vol. 83, no. 1, pp. 100 – 103, 1999.

[17] C. J. Garasi, D. E. Bliss, T. A. Mehlorn, B. V. Oliver, A. C. Robinson, G. S. Sarkisov, "Multi–dimensional high energy density physics modelling and simulation of wire array Z–pinch physics," *Physics of Plasmas*, vol. 11, no. 5, pp. 2729, 2004.

[18] G. Rodríguez Prieto, L. Bilbao, and M. Milanese, "Temporal distribution of the electrical energy on an exploding wire," *Laser and Particle Beams*, vol. 34, no. 02, pp. 263–269, 06 2016. [Online]. Available: http://journals.cambridge.org/article_S0263034616000069

[19] L. Bilbao and H. Bruzzone, "Comments on "the time evolution of the resistances and inductances of the discharges in a pulsed gas laser through its current waveforms"," *IEEE Transactions on Plasma Science*, vol. 26, no. 1, pp. 119–121, Feb 1998.

[20] C. Nash and W. McMillan, "On the mechanism of exploding wires," *Physics of Fluids (1958-1988)*, vol. 4, no. 7, pp. 911–917, 1961.

[21] A. W. DeSilva and H.-J. Kunze, "Experimental study of the electrical conductivity of strongly coupled copper plasmas," *Physical Review E*, vol. 49, pp. 4448–4454, May 1994. [Online]. Available: http://link.aps.org/doi/10.1103/PhysRevE.49.4448

[22] A. Grinenko, Y. E. Krasik, S. Efimov, F. G., and V. T. Gurovich, "Nanosecond time scale, high power electrical wire explosion in water," *Physics of Plasmas*, vol. 13, no. 4, p. 042701, 2006.

[23] H. Bruzzone, H. Kelly, and C. Moreno, "On the effect of finite closure time of switches in electrical circuits with fast transient behavior," *American Journal of Physics*, vol. 57, no. 1, pp. 63 – 66, 1989. [Online]. Available: http://scitation.aip.org/content/aapt/journal/ajp/57/1/10.1119/1.15872

[24] B. E. Fridman, P. Persephonis, V. Giannetas, A. Ioannou, J. Parthenios, and C. Georgiades, "Comments on "the time evolution of the resistances and inductances of the discharges in a pulsed gas laser through its current waveforms" [with reply]," *IEEE Transactions on Plasma Science*, vol. 25, no. 4, pp. 799 – 801, Aug 1997.

[25] R. A. Matula, "Electrical resistivity of copper, gold, palladium, and silver," *Journal of Physical and Chemical Reference Data*, vol. 8, no. 4, pp. 1147 – 1298, 1979. [Online]. Available: http://scitation.aip.org/content/aip/journal/jpcrd/8/4/10.1063/1.555614

[26] L. Bilbao, "A three-dimensional finite volume arbitrary lagrangian-eulerian code for plasma simulations," *AIP Conference Proceedings*, vol. 875, no. 1, pp. 467 – 472, 2006. [Online]. Available: http://scitation.aip.org/content/aip/proceeding/aipcp/10.1063/1.2405990

ACKNOWLEDGMENT

This study has been partially supported by the Ministerio de Energía y Competitividad of Spain (ENE2013-45661-C2-1-P) and Junta de Comunidades de Castilla-la Mancha (EII-2014-008-P). Authors would like to thank Prof. Roberto Piriz for comments and suggestions.